Biochemistry

 Volume 38, Number 21 May 25, 1999

Articles

Ligand-Induced Conformational Changes in Lactose Repressor: A Phosphorescence and ODMR Study of Single-Tryptophan Mutants†

Andrzej Ozarowski,‡ Jennifer K. Barry,§ Kathleen S. Matthews,*,§ and August H. Maki*,‡

Department of Chemistry, University of California, Davis, California 95616, and Department of Biochemistry and Cell Biology, Rice University, Houston, Texas 77005-1892

Received February 2, 1999; Revised Manuscript Received April 1, 1999

ABSTRACT: Phosphorescence and optically detected magnetic resonance (ODMR) measurements are reported on four single-tryptophan mutants of *lac* repressor protein from *Escherichia coli*: H74W/Wless, W201Y, Y273W/Wless, and F293W/Wless, where Wless represents a protein background containing the double mutation W201Y/W220Y. The single-tryptophan residues are located in the protein core region, either in the monomer−monomer interface of the tetrameric protein or in the region of the inducer binding cleft. Inducer binding elicits large changes in the energy (0,0-band wavelength shifts) and zero-field splitting energies (ZFS) of the triplet states for each of the mutant proteins except W201Y which exhibits more modest effects. F293W/Wless exists in two distinguishable conformations, only one of which appears to be sensitive to the presence of inducer. These effects of inducer binding can be attributed to a conformational change that alters specific polar interactions that occur at each affected tryptophan site. Changes in the tryptophan triplet state indicator depend on the existence of specific polar interactions that are altered by local atomic relocations.

The *lac* repressor protein is a negative regulator of *lac* operon structural genes by means of high-affinity binding with the *lac* operator sequence (*1*). When complexed with the natural inducer sugar, allolactose, a metabolite of lactose (*2*), the affinity of *lac* repressor protein for the operator is reduced severely, making nonspecific DNA binding competitive with *lac* operator binding and thereby allowing transcription of the *lac* structural genes to take place (*1*, *3*). The ability of one ligand to influence the binding affinity of a second ligand is a result of ligand-induced alterations in the protein structure. Conformational changes in the protein that are associated with ligand binding have been detected by a variety of methods, including altered accessibility of residues to chemical modification, spectral changes in tryptophan and tyrosine residues, and other biophysical techniques (reviewed in ref *4*). The X-ray crystallographic structures of the different ligand-bound states of *lac* repressor identify the regions of the protein which participate in these conformational changes (*5*). Structural rearrangements that occur mainly between the different ligand-bound states are found primarily in the N-subdomain of the core region in the monomer−monomer interface (*5*, *6*).

The observed similarity between the X-ray crystallographic structures of the unliganded and inducer-bound protein is inconsistent with previous biochemical and biophysical data that demonstrate conformational shifts associated with

† Support for this project was provided by grants from the NIH to A.H.M. (ES 02662) and K.S.M. (GM 22441) and from the Robert A. Welch Foundation (C-576) to K.S.M.

* To whom correspondence should be addressed. A.H.M.: phone, (530) 752-6471; fax, (530) 752-8995; e-mail, maki@indigo.ucdavis.edu. K.S.M.: phone, (713) 527-4871; fax, (713) 737-6149; e-mail, ksm@bioc.rice.edu.

‡ University of California.

§ Rice University.

10.1021/bi990242f CCC: $18.00
Published on Web 04/29/1999

inducer binding (*4*, *5*). Structural changes between the free and inducer-bound conformations of the protein are reflected in alterations in physical properties and in spectroscopic properties of side chains dispersed throughout the structure (*4*, *7*). One rationale for these differences between crystallographic data and solution studies is that the crystal structures provide a picture of the final conformations that the protein can assume when bound to its ligands, in comparison to the dynamic processes or the potential intermediate structures involved in the transitions between conformations. To explore this possibility, Barry and Matthews (*7*) studied the influence of ligand binding on the fluorescence characteristics of the tryptophan residue in a number of single-tryptophan mutants of *lac* repressor protein. In these studies, the effect of the mutation on operator and inducer binding affinity was assessed, as well as the influence of ligand binding on the local environment of single tryptophan residues located at various sites in *lac* repressor. The effect of ligand binding on the quenching efficiency by neutral and ionic quenchers of tryptophan fluorescence was monitored for each of the single-tryptophan mutants. In addition to W201Y and W220Y, in which the tryptophan residue is located at one of the native positions (W220 and W201, respectively), single tryptophans were introduced at a series of sites in a doubly mutated tryptophan-free background (both W201 and W220 mutated to tyrosine, referred to as Wless[1]).

Fluorescence properties of single tryptophans incorporated at various sites in proteins provide valuable information about local environment and conformational changes induced by ligand binding. Other spectroscopic methods, many far less widely applied, have the potential of providing complementary insight into structure. Among these are tryptophan phosphorescence and the associated optical detection of magnetic resonance (ODMR) spectroscopy. These methods rely on the production of the excited triplet state of the tryptophan residue by optical pumping in the singlet manifold followed by intersystem crossing to the triplet states (*8*). The phosphorescence spectrum is shifted and broadened by the local environment, reflecting the degree of solvent exposure relative to hydrophobic interactions with polarizable residues (*9*). In addition, the triplet state is paramagnetic, and the spin degeneracy is removed by inter-electron magnetic dipole−dipole interactions even in the absence of an applied magnetic field. Magnetic resonance transitions between the triplet sublevels are detected by monitoring the phosphorescence, yielding ODMR spectra (*10*, *11*). The zero-field splitting (ZFS) energies and the ODMR bandwidths are influenced by the local environment and may be used to monitor conformational changes induced in *lac* repressor by ligand binding. Previously, phosphorescence and ODMR spectroscopy have been used to examine wild type *lac* repressor protein, W201Y, and W220Y (*12*).

We report in this paper the results of phosphorescence and ODMR measurements on several single-tryptophan mutants studied earlier (*7*) by fluorescence methods, H74W/Wless, W201Y, Y273W/Wless, and F293W/Wless. The tryptophans selected in this study are located in the core domain. A representation of the core domain of *lac* repressor protein is shown in Figure 1, which indicates the location of W220, and the residues replaced by tryptophan in the Wless single-tryptophan mutants examined in this work. The tryptophan residues are associated with the inducer binding pocket (W201Y and F293W/Wless) or the monomer−monomer interface (H74W/Wless) or lie in the vicinity of the inducer binding pocket (Y273W/Wless). These residues are partially exposed to solvent, on the basis of fluorescence quenching studies carried out previously (*7*). In contrast with exterior solvent-exposed tryptophans, their fluorescence properties are altered by inducer binding. The data presented provide additional information about the local environment at these specific tryptophan sites and about the influence of inducer binding at each site.

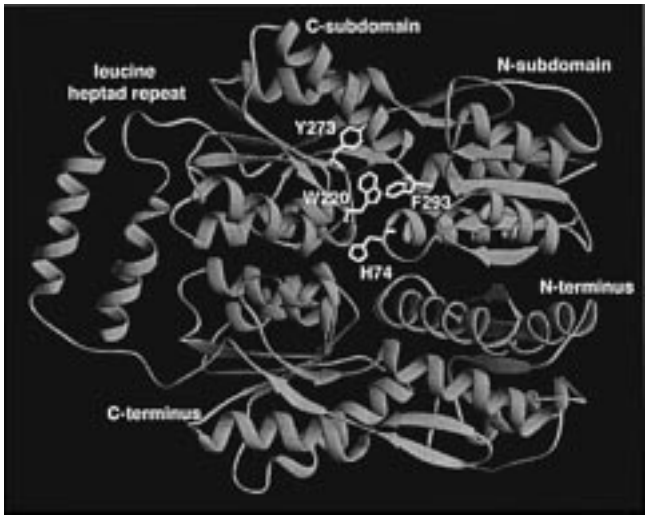

FIGURE 1: Lactose repressor core domain structure. The structure was derived from PDB file 1LBH (*5*), which contains the coordinates of the repressor complexed with IPTG. Only one dimer of the tetrameric structure is shown. The wild type side chains are shown in one of the monomers only for the sites examined in this study: H74, W220, Y273, and F293. The figure was drawn with Ribbons, version 2.63 (*29*). The N- and C-termini, the N- and C-subdomains, and the leucine heptad repeat sequences that form the tetramer are labeled.

MATERIALS AND METHODS

Mutagenesis. Protein samples were prepared in the Rice laboratories. Mutations in the *lac* repressor gene were generated in the pAC1 plasmid (*13*) using the method of Kunkel (*14*). The two native tryptophans in *lac* repressor (residues 201 and 220) have been converted to tyrosine and characterized individually (*15*, *16*). The pAC1 plasmid containing the *lac* repressor gene with the W220Y mutation (*15*) was used to produce the W201Y/W220Y double mutant. Mutagenesis to produce the single-tryptophan repressors was performed using uracil-containing template with the W201Y/W220Y mutation. Protein purification was carried out as described previously (*7*, *17*, *18*).

Preparation of Protein Samples for Spectroscopy. The single-tryptophan mutants of *lac* repressor protein were dialyzed into 0.1 M potassium phosphate (KP) buffer (pH 7.4) containing ethylene glycol (EG, 30% v/v) as a cryosolvent. The concentrations were ~1 mM in monomer.

[1] Abbreviations: *D* and *E*, triplet-state zero-field splitting parameters; EEDOR, electron−electron double resonance; EG, ethylene glycol; KP, potassium phosphate; MIDP, microwave-induced delayed phosphorescence; ODMR, optical detection of magnetic resonance; Wless, doubly mutated (W201Y/W220Y) tryptophan-free lactose repressor protein from *Escherichia coli*; ZFS, zero-field splittings.

Samples were stored at −80 °C until they were shipped with dry ice to the Davis laboratories for spectroscopic measurements. Complexing with the isopropyl β-D-thiogalactoside (IPTG) inducer was carried out by adding 20 μL of a 1 M solution of IPTG in the pH 7.4 KP buffer containing 30% v/v EG to 75−100 μL of a protein solution to produce a ratio of ∼200:1 (IPTG/monomer). Mixtures were incubated at room temperature for 1−2 h. Samples (∼50 μL) were loaded into 1 mm inside diameter suprasil quartz tubes for spectroscopic measurements.

Phosphorescence and ODMR Measurements. These measurements were carried out at a temperature of 1.2 K, achieved by immersing the sample in liquid He whose vapor pressure was reduced by a mechanical pump. The phosphorescence/ODMR spectrometer has been described previously (*19*). All spectra were obtained using photon counting; signal averaging of the ODMR spectra was carried out in a multichannel analyzer. The sample was excited by a 100 W high-pressure Hg arc lamp filtered with a monochromator using a 16 nm bandwidth along with a glass ultraviolet cutoff filter when required for excitation at the red edge of the absorbance. Slow-passage ODMR spectra were obtained by monitoring the peak of the prominent tryptophan 0,0-phosphorescence band using a 3.2 nm monochromator bandwidth. The spectra were obtained at several microwave sweep rates and corrected for the transient effects of rapid passage by a previously described procedure (*19*). This procedure assumes a symmetric Gauss-shaped ODMR band having center frequency ν_0 and a half-width at half-maximum intensity of $\nu_{1/2}$. The effects of rapid microwave passage on the Gaussian are fitted to the observed band by a nonlinear least-squares procedure using ν_0 and $\nu_{1/2}$ as two of the fitted variables. Standard deviations in ν_0, and $\nu_{1/2}$, were calculated from the variance of the data sets. The very weak high-frequency ODMR transition ($D + E$) was enhanced using the electron−electron double-resonance (EEDOR) method, saturating the low-frequency ($D - E$) transition. The saturating microwaves were frequency-modulated at a low audio frequency over the entire inhomogeneously broadened $D - E$ band to saturate this transition completely. This band was absent in the EEDOR spectrum, confirming saturation of this transition. The zero-field splitting parameters were calculated from the observed ν_0 using the following equations:

$$D = {}^1/_2[\nu_0(D - E) + \nu_0(D + E)] \quad (1)$$

$$E = {}^1/_4[\nu_0(D + E) + \nu_0(2E) - \nu_0(D - E)] \quad (2)$$

The choice of the ZFS parameters arises from the symmetry-based assignment of *z* as the out-of-plane principal axis. The in-plane *x*- and *y*-axes are not determined by symmetry, but the axis assigned as *x* is found to be nearly normal to the double bond of indole (*11*). The large value of *E* in tryptophan, due to significant spin density in the double bond, yields an "unconventional" energy level structure in which the $T_x \leftrightarrow T_y$ transition frequency, ν_0 (2*E*), lies between the other two.

Microwave-induced delayed phosphorescence (MIDP) transients (*20*) were analyzed globally as described previously (*21*) to obtain the individual sublevel decay constants, k_i, their relative radiative rate constants, R_{ji}, and the inter-sublevel spin−lattice relaxation rate constants, W_{ji} ($i, j = x, y, z$).

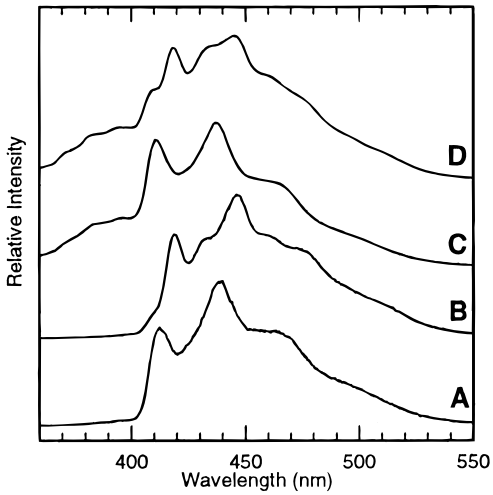

FIGURE 2: Phosphorescence spectra of H74W/Wless at 1.2 K. Spectra A and B are for the free protein and its IPTG complex excited at 313 nm through a WG 305-2 filter, respectively. Spectra C and D are for the free protein and its IPTG complex, respectively, excited at 297 nm through a WG 295-1 filter.

RESULTS

Phosphorescence and ODMR of H74W/Wless and Its IPTG Complex. The phosphorescence spectra of H74W/Wless and its IPTG complex are compared in Figure 2. Using red-edge excitation, a clean, structured tryptophan emission is observed from the free protein with a 0,0-band peaking at 413 nm (Figure 1A). The IPTG complex, using the same red-edge excitation conditions, produces the spectrum shown in Figure 1B; the prominent 0,0-band of tryptophan is red-shifted to 419 nm. When the excitation wavelength is shifted well into the protein absorption band, the phosphorescence spectra of H74W/Wless and its IPTG complex appear as in spectra C and D of Figure 2, respectively. Both spectra reveal tyrosine phosphorescence that appears as a broad emission to the blue of 400 nm. The blue shift of the 0,0-band of H74W/Wless from 413 to 411 nm should be noted. This shift is the result of heterogeneity of the tryptophan site due to random polar interactions and is not found in completely buried residues (*22*). The IPTG complex of H74W/Wless exhibits tyrosine emission, but also a minor peak at 411 nm. We assign the latter as the 0,0-band of residual uncomplexed H74W/Wless. The assignment is supported by comparison of ODMR spectra of samples of the protein and its IPTG complex monitored at 411 nm (data not presented).

The slow-passage ODMR spectra of H74W/Wless and its complex with IPTG are compared in Figure 3. As indicated in the previous section, the ODMR band center frequencies, ν_0, and bandwidths, $\nu_{1/2}$, were obtained by fitting the individual responses to an algorithm (*19*) that introduces the effects of microwave fast passage on the assumed Gauss-shaped bands. An example of this procedure is illustrated in Figure 4 for H74W/Wless. It should be noted that the peak positions of the fitted responses are displaced to higher frequencies relative to the ν_0 of the Gaussian bands as a result of the rapid passage effects. The ODMR center frequencies and bandwidths of the Gaussian bands obtained by using this procedure are listed in Table 1, along with the calculated

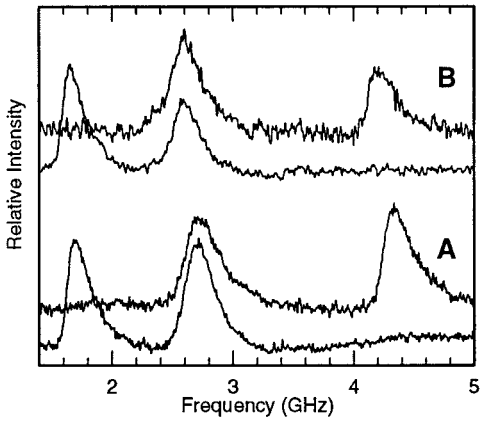

FIGURE 3: ODMR spectra of free H74W/Wless observed at 1.2 K by (A) monitoring the 413 nm emission band of the free protein and (B) monitoring the 419 nm emission band of the IPTG complex. Excitation was at 302 nm using a WG 305-2 filter in each case. EEDOR spectra with saturation of the $D - E$ transition are shown above the normal spectra.

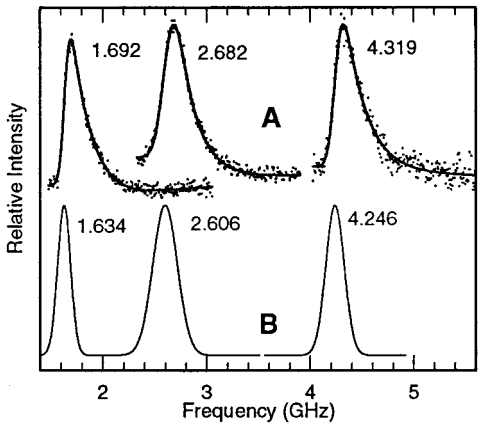

FIGURE 4: Fast passage effect in the ODMR spectra of H74W/Wless. (A) Experimental spectra (points) recorded separately for the $D - E$, $2E$, and $D + E$ transitions with simulated responses fitted according to the method described in ref *19*. The $D + E$ response is obtained while saturating the $D - E$ band. The microwave frequency increases at 79 MHz/s for each response. The Gaussian bands predicted at zero sweep rate are shown in spectrum B. Peak frequencies are given in gigahertz.

ZFS parameters, D and E. Significant changes in the ODMR band frequencies and considerable narrowing of the bandwidths occur when IPTG is bound. Monitoring the phosphorescence of H74W/Wless at 360 nm when exciting at 280 nm, well into the protein absorption, yields three ODMR transitions characteristic of the tyrosine triplet state (*23*) (2.35, 3.53, and 5.71 GHz, uncorrected for fast passage effects).

The triplet-state kinetic and relative radiative rate constants of H74W/Wless and its IPTG complex obtained from global analysis of MIDP data are listed in Table 2. The kinetic parameters observed previously (*21*) for tryptophan in EG/water are included for comparison. All kinetic parameters of W74 in both the protein and its IPTG complex are close to those of solvent-exposed free amino acid, except that the k_x values are significantly larger.

W201Y and Its IPTG Complex. The phosphorescence of W201Y was found to be similar to that reported previously (*12*). Careful measurement of the 0,0-bands reveals a minor blue shift (409.8 to 408.4 nm) upon complex formation, also reported previously (*12*). The slow passage ODMR revealed small changes in the band peak frequencies and widths upon complex formation (Table 1). These small differences were not detected in the earlier study (*12*) in which correction of the line shape for fast passage effects (*19*) was not employed. The kinetic parameters listed in Table 2 are similar, as for the H74W/Wless protein, to those of the free amino acid except for an increase of k_x. An increase in W_{yz} is induced by IPTG complex formation.

Y273W/Wless and Its IPTG Complex. In contrast with the spectrum of H74W/Wless where a large red shift is found upon binding IPTG, W273 of Y273W/Wless undergoes a blue shift of its 0,0-band from 415 to 413 nm (Table 1). The phosphorescence vibronic bands also narrow considerably in the IPTG complex (spectrum not shown), indicating a decrease in the heterogeneity of the environment of W273. Large changes in the ν_0, and $\nu_{1/2}$, of the ODMR bands are induced by IPTG binding. These data are presented in Table 1. The slow passage ODMR spectra of Y273W/Wless and its IPTG complex are compared in Figure 5. Consistent with the phosphorescence, the ODMR bands become much narrower in the IPTG complex, indicating a more homogeneous local environment. The D parameter is unusually small in Y273W/Wless; both D and E undergo large increases when IPTG is bound. As found in H74W/Wless and W201Y, the value of k_x is significantly larger than is found for the free amino acid; W_{yz} increases, as with W201Y, when IPTG is bound (Table 2).

F293W/Wless and Its IPTG Complex. Unlike the other proteins examined, this single-tryptophan mutant exhibits phosphorescence from two distinguishable sites. Figure 6A shows the phosphorescence spectrum of F293W/Wless, clearly revealing two 0,0-bands at 408 and 415.7 nm. Addition of IPTG alters the relative intensity of the two 0,0-bands (Figure 6B) and introduces about a 1 nm blue shift of the 408 nm peak. Slow passage ODMR spectra of F293W/Wless, monitoring each of the 0,0-band peaks separately, differ significantly (Table 1). The E parameter is 170 MHz larger for the red-shifted tryptophan site. Analysis of the slow passage ODMR spectra of the IPTG complex of F293W/Wless is not reliable because of interference from free protein even with a 200:1 ratio of IPTG to monomer. The affinities of both H74W/Wless and F293W/Wless for inducer are reduced by 2−3 orders of magnitude relative to that of the wild type, whereas the affinity of W201Y is comparable to that of the wild type and that of Y273W/Wless reduced by less than 1 order of magnitude (*7*). Thus, quantitative binding of IPTG could be achieved only with W201Y and Y273W/Wless. Qualitatively, however, large changes in the ODMR spectrum of F293W/Wless are found with added IPTG when monitoring the blue-shifted peak near 407 nm, while little change, if any, is observed by monitoring the peak near 415 nm. The ODMR spectra of F293W/Wless with and without added IPTG are compared at both monitored peaks in Figure 7. When the protein was monitored at the blue-shifted site, IPTG binding induces about a 250 MHz shift of the $2E$ band to higher frequency, a smaller shift of the $D - E$ band to a lower frequency, and a narrowing of both ODMR bands (compare spectra A and B of Figure 7). When the protein was monitored at the red-shifted site, no noticeable change in the ODMR spectrum is found upon addition of IPTG (compare spectra C and D of Figure 7). The kinetic

Table 1: Zero-Field Splitting Parameters for Free Proteins and Their Complexes with IPG

sample, λ (nm) at 1.2 K	$\lvert D\rvert - \lvert E\rvert$[a]		$2\lvert E\rvert$[a]		$\lvert D\rvert + \lvert E\rvert$[a]			
	ν_0 (GHz)	$\nu_{1/2}$ (MHz)	ν_0 (GHz)	$\nu_{1/2}$ (MHz)	ν_0 (GHz)	$\nu_{1/2}$ (MHz)	$\lvert D\rvert$ (GHz)	$\lvert E\rvert$ (GHz)
W in EG/H_2O (406.7)[b]	1.763(3)	58(1)	2.514(10)	146(6)	4.250(7)	81(4)	3.01	1.25
H74W/Wless (413)	1.634(4)	48(1)	2.606(3)	91(5)	4.246(7)	68(2)	2.94	1.30
IPTG complex (419)	1.594(3)	42.2(3)	2.503(3)	82(2)	4.101(2)	56(6)	2.85	1.25
W201Y (410)	1.719(1)	42.8(7)	2.436(2)	97(2)	4.145(2)	73(2)	2.93	1.22
IPTG complex (408.5)	1.745(1)	38.7(3)	2.413(4)	96(1)	4.146(2)	64(1)	2.95	1.20
Y273W/Wless (415)	1.493(2)	41(1)	2.508(3)	73(3)	4.083(3)	65(1)	2.79	1.27
IPTG complex (413)	1.583(1)	27(1)	2.675(2)	58(3)	4.259(1)	47(1)	2.92	1.34
F293W/Wless (415)	1.586(1)	35(3)	2.693(9)	86(11)	–	–	2.93	1.35
F293W/Wless (408)	1.744(4)	65(9)	2.364(5)	125(3)	–	–	2.93	1.18

[a] Standard errors (σ_e) in the last digit given in parentheses. [b] Data from ref *30*.

Table 2: Kinetic and Radiative Parameters

sample	k_x (s^{-1})[a]	k_y (s^{-1})[a]	k_z (s^{-1})[a]	R_{zx}[a]	R_{yx}[a]	W_{xy} (s^{-1})[a]	W_{xz} (s^{-1})[a]	W_{yz} (s^{-1})[a]	τ (s)[b]
W (EG/H_2O)[c]	0.306(9)	0.102(5)	0.000(4)	0.000(1)	0.128(7)	0.013(3)	0.040(5)	0.044(1)	6.8
H74W/Wless	0.375(7)	0.113(4)	0.000(3)	0.000(8)	0.108(6)	0.008(3)	0.036(4)	0.039(4)	6.1
IPTG complex[c]	0.40(1)	0.127(6)	0.005(5)	0.02(1)	0.11(1)	0.010(4)	0.031(6)	0.048(7)	5.6
W201Y free	0.323(7)	0.090(3)	0.004(2)	0.000(8)	0.015(6)	0.025(2)	0.031(4)	0.0498(4)	6.7
IPTG complex	0.35(1)	0.096(5)	0.003(3)	0.00(1)	0.00(1)	0.020(4)	0.023(5)	0.0711(5)	6.7
Y273W/Wless	0.35(1)	0.114(5)	0.000(3)	0.01(1)	0.044(8)	0.033(4)	0.033(6)	0.065(1)	6.4
IPTG complex	0.35(2)	0.106(9)	0.000(4)	0.00(2)	0.02(1)	0.034(7)	0.04(1)	0.091(1)	6.5
F293W/Wless[d]	0.38(8)	0.12(4)	0.00(2)	0.00(2)	0.00(2)	0.00(2)	0.04(4)	0.044(4)	–[e]
F293W/Wless[f]	0.30(2)	0.12(1)	0.000(6)	0.00(2)	0.13(2)	0.00(1)	0.04(1)	0.046(1)	6.8[g]

[a] Standard errors (σ_e) in the last digit given in parentheses. [b] Lifetimes were measured at 77 K. [c] Data from ref *21*. [d] Red-shifted site. [e] The lifetime was not determined due to the interference of the blue-shifted site. [f] Blue-shifted site. [g] Lifetime measured at 4.2 K.

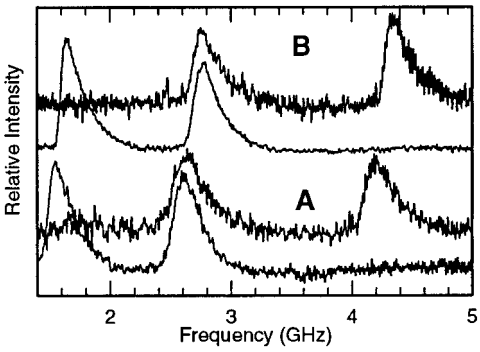

FIGURE 5: ODMR spectra of Y273W/Wless observed at 1.2 K by (A) monitoring the emission of free protein at 415 nm with excitation at 313 nm using a WG 305-2 filter and (B) monitoring emission of the IPTG complex at 413 nm with excitation at 302 nm using a WG 305-2 filter. EEDOR spectra with saturation of the $D - E$ transition are shown above the normal spectra.

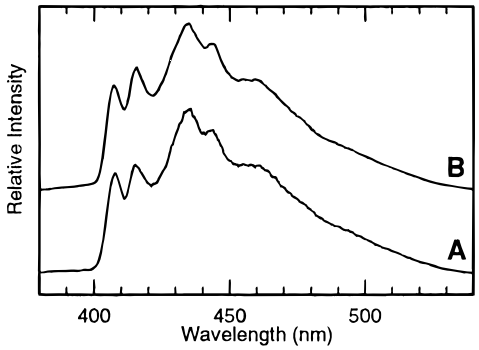

FIGURE 6: Phosphorescence of F293W/Wless observed at 1.2 K with excitation at 302 nm using a WG 305-2 filter: (A) free F293W/Wless and (B) F293W/Wless complexed with IPTG.

parameters of tryptophan at the blue-shifted site of uncomplexed F293W/Wless are close to those of the free amino acid, while the red-shifted site has an increased k_x (Table 2).

DISCUSSION

This work utilizes the sensitivity of the triplet state of tryptophan to changes in the local environment to detect conformational changes in protein structure. Four mutant *lac* repressor proteins, each containing a single tryptophan residue, were selected to monitor conformational changes that occur upon binding inducer. For perspective on the methodology, the triplet energy and ZFS values are altered only to the extent that a conformational change affects the charge distribution as viewed by the indole chromophore. The triplet-state energy and the ZFS are affected by the environment via the interaction of the internal electrons with the local electrical charge distribution. Tryptophan residues subjected to large specific polar interactions should be most strongly affected by conformational changes that involve changes in local structure.

H74W/Wless. H74 is located in the N-subdomain in the monomer−monomer interface of *lac* repressor near the inducer binding site (Figure 1) (*5*). It has been suggested (*5*, *7*) that the electrostatic interaction of H74 across the interface with D278 in the C-subdomain of the monomer partner may be critical for inducer diminution of operator affinity. Substitution of tryptophan at this site in the Wless background greatly reduces the affinity for inducer and leads to an extremely stable operator complex that is less responsive to the presence of inducer (*7*). We find that H74W/Wless binds inducer at a concentration of 200 mM, but incompletely (Figure 2).

Previous studies demonstrated that inducer binding altered the fluorescence properties of the tryptophan at residue 74, with a blue shift of the fluorescence emission spectrum and decreased exposure to quenching by iodide (*7*). These results

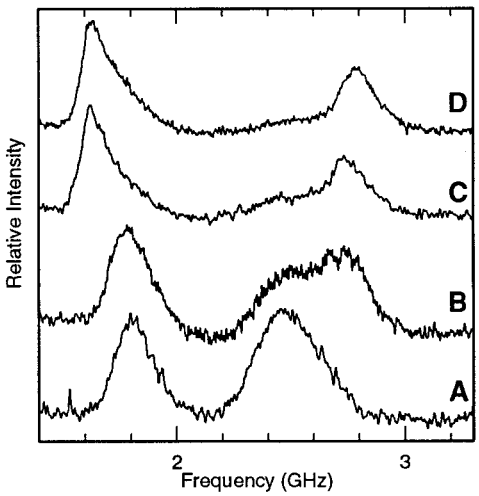

FIGURE 7: ODMR spectra of 293W/Wless observed at 1.2 K. (A) Free protein-monitoring blue-shifted variety at 408 nm. (B) IPTG complex-monitoring blue-shifted variety at 406 nm. (C) Free protein-monitoring red-shifted variety at 416 nm. (D) IPTG complex-monitoring red-shifted variety at 415 nm. The excitation wavelength was 302 nm using a WG 305-2 filter in each case.

indicated that the tryptophan at residue 74 is less exposed to solvent when the inducer binding pocket is occupied. The conclusions from the phosphorescence studies are similar; the environment around W74 is altered by inducer binding, and consequently, the indole side chain becomes less accessible to solvent. The ZFS energies of W74 differ significantly from those of free solvent-exposed tryptophan, and the bandwidths are considerably narrower (Table 1), suggesting a relatively structured environment. The 0,0-band is shifted more than 6 nm to the red relative to that of solvent-exposed tryptophan, and k_x is 25% larger. IPTG binding produces an additional 6 nm red shift (a total red shift of >12 nm relative to that of solvent-exposed tryptophan) and the narrowing of phosphorescence and ODMR bandwidths. Both *D* and *E* parameters are reduced, consistent with an overall expansion of the excited state electron distribution.

Tryptophan phosphorescence shifted this far to the red is very unusual. The tryptophan 0,0-band is red shifted by aromatic stacking interactions, and values up to 419−420 nm have been found for complexes of HIV-1 nucleocapsid protein (NCp7) with $d(IT)_2$ and $d(IT)_4$ (*24*). In these stacked complexes, however, k_x is twice the size of that found for solvent-exposed tryptophan, rather than only 30% larger (Table 2). The only comparable red-shifted tryptophan 0,0-band found thus far in the absence of aromatic stacking (420 nm) was assigned (*25*) to W84 of yeast glyceraldehyde-3-phosphate dehydrogenase. This red shift for the dehydrogenase was ascribed to effects from a nearby protonated histidine (H108) hydrogen bonded with aspartate (D94), but at a sufficient distance to avoid quenching W84. If a similar arrangement of electrical charge is present near W74 in H74W/Wless, possibly involving the nearby residue D278, changes in this strong polar interaction could account for the large effects of inducer binding on the triplet state. Whatever the cause, the strong influence of IPTG binding on the triplet state properties of W74 in H74W/Wless points to a major conformational change affecting W74 when inducer is bound, in agreement with earlier fluorescence results (*7*). In this mutant, the lack of a significant decrease in operator affinity when bound to inducer may indicate that this conformational change is not propagated beyond the inducer binding region.

W201Y. W220, the single tryptophan residue in this mutant, is part of a hydrophobic patch, also including F293, that participates in inducer binding (*5*, *6*). Consequently, mutation of W220 to tyrosine results in a 10-fold decrease in inducer binding affinity. The position of the phosphorescence 0,0-band is consistent with essentially a polar, nonpolarizable environment (*9*); the relatively narrow ODMR bandwidths suggest a more homogeneous local environment than is found with complete solvent exposure. The ODMR frequencies also differ significantly from those of the solvent-exposed amino acid. All of these data are consistent with a partially shielded residue. Extensive fluorescence studies have determined that inducer binding alters the fluorescence properties of the tryptophan at this position. The fluorescence of W201Y (W220) undergoes a sizable blue shift when IPTG is bound; W220 is partially exposed, and inducer binding reduces somewhat the accessibility to quenchers (*7*). IPTG binding causes only relatively minor changes of the triplet-state properties of W220, in agreement with earlier work (*12*). Any conformational changes in *lac* repressor associated with inducer binding that involve the hydrophobic patch are felt only weakly at the W220 site.

Y273W/Wless. Y273 is located near the inducer binding cleft in the C-subdomain (*5*, *6*). Although this residue is not located in either ligand binding site, the Y273W/Wless mutant displays a 3−4-fold reduction in the affinity for both operator and inducer (*7*), indicating that this region of the protein has some involvement in ligand binding. W273 appears to be shielded from the surface, since its fluorescence undergoes almost no quenching by iodide and is only partially accessible to acrylamide and thallium quenchers. On the basis of ODMR bandwidths, W273 in Y273W/Wless has the most homogeneous environment of the set of *lac* repressor mutants in our study. The 0,0-band wavelength of Y273W/Wless is in the range characteristic of a tryptophan residue located either in a polarizable hydrophobic environment (*9*) or in an environment in which specific polar interactions with the tryptophan dipole moment fortuitously favor the excited triplet state rather than the ground state (*26*). The ZFS *D* parameter of Y273W/Wless is unusually small as a result of expansion of the electron distribution, leading to a greater interelectron separation and reduced dipole−dipole interaction. This expansion can result from either of the causes of the red shift mentioned above, or the combined effect of both. The partial accessibility to quenchers suggests that W273 is not buried in a hydrophobic environment, and thus, polar interactions may contribute to the anomalous ZFS. Furthermore, in contrast with W273, tryptophan residues that are buried in hydrophobic environments tend to have significantly increased values of the *E* parameter relative to those of solvent-exposed residues. This situation is the case for the W220Y *lac* repressor mutant, for instance, in which W201 is a buried residue ($D = 2.99$, $E = 1.37$ GHz) (*12*).

Inducer binding alters the fluorescence properties of the tryptophan at the Y273 site. When inducer is bound, the accessibility of this residue to acrylamide quenching increases while that to thallium quenching decreases (*7*). Inducer binding also shifts the fluorescence emission spectrum to shorter wavelengths. Changes in this region in response to

inducer are also detected when the tryptophan environment is monitored using phosphorescence. The significant decrease in ODMR bandwidths upon binding inducer suggests a further decrease in local heterogeneity compared to that of the unliganded environment (Table 1). The ZFS energies of Y273W/Wless change significantly when the inducer is bound; *D* and *E* increase to values that are more closely consistent with a simple polarizable environment (Table 1). The blue shift of the 0,0-band that occurs on inducer binding supports the suggestion that the initial red-shifted position of the Y273W/Wless phosphorescence is influenced by polar interactions that selectively stabilize the excited triplet-state dipole moment relative to that of the ground state. Conformational changes at this site that accompany inducer binding reduce these interactions, leading to the observed blue shift of the phosphorescence and a more normal ZFS pattern.

F293W/Wless. F293 is located in the inducer binding pocket, along with W220 (*5*, *6*). Substitution of F293 with alanine or tyrosine greatly reduces the inducer binding affinity (*27*), while replacement with tryptophan leads to a 100-fold decrease in the inducer affinity as revealed by an in vitro competitive binding assay (*7*). In previous quenching studies, the accessibility to quencher depended upon the nature of the quencher; W293 was quenched by iodide less efficiently than W220, but the reverse was the case for acrylamide and thallium quenching (*7*). At cryogenic temperatures, this sample of F293W/Wless was found to contain two structural varieties that are distinguished by widely differing triplet-state properties of W293 (Figure 4 and Tables 1 and 2). With a focus on the blue-shifted structural variety of F293W/Wless, the ODMR bands are as broad as those of solvent-exposed free tryptophan (Table 1), indicating considerable local heterogeneity. Both *D* and *E* are considerably smaller than those of free tryptophan, however, indicating the presence of specific polar interactions with the surrounding structure. The short wavelength of the 0,0-band, near that of solvent-exposed tryptophan, indicates that local charges are positioned to stabilize the ground state dipole moment of tryptophan relative to that of the excited state. This observation is in contrast with the situation encountered with Y273W/Wless, where polar interactions preferentially stabilize the excited state.

Previously, changes in the tryptophan environment at the F293 site upon inducer binding were detected by thallium and iodide quenching, as well as changes in the fluorescence emission spectra. Of the two structural varieties of F293W/Wless that we observe, only the one with blue-shifted origin (408 nm) is affected by adding inducer (Figure 5). Inducer binding is accompanied by a large increase in the ZFS *E* parameter. Binding of IPTG also leads to a small blue shift of the 0,0-band of this variety to 407 nm. Although we are not able to analyze the ODMR bands accurately because of interference from uncomplexed protein, the ZFS parameters of the complex can be estimated from the positions of the relatively narrow $D - E$ and $2E$ peaks in Figure 5B; $D = 3.06 \pm 0.03$ GHz, and $E = 1.35 \pm 0.02$ GHz. The large values of both *D* and *E* suggest a repulsive environment for the triplet-state electrons that induces contraction of the charge distribution. Little or no changes in the red-shifted variety are observed when the inducer is added at a concentration of 200 mM (spectra A and B of Figure 5). Either this form of F293W/Wless does not bind inducer, or inducer binding by the red-shifted variety has only a minor affect on the W293 triplet state.

It is important to consider the potential effects of our experimental conditions on protein structure and on ligand binding properties. Whereas the fluorescence measurements (*7*) on these samples were taken in aqueous buffer at ambient temperatures, the measurements reported here were taken at cryogenic temperatures with the addition of 30% (v/v) EG as a cryosolvent. These extreme conditions are necessary to observe ODMR signals with measureable intensity (*10*, *11*). Previous ODMR and phosphorescence measurements reveal structural changes in ribonuclease T1 from *Aspergillus oryzae* at cryogenic temperatures in the presence of added EG, but these do not become noticeable below 60% (v/v) EG (*28*). With the exception of one structural form of F293W/Wless, each *lac* repressor mutant that was studied reveals effects showing that IPTG binding occurs. Binding is incomplete in the mutants whose affinity for inducer was shown by fluorescence to be severely reduced (H74W/Wless and F293W/Wless, blue-shifted structure), while binding is stoichiometric in the mutants exhibiting good binding affinity in the fluorescence studies (W201Y and Y273W/Wless) (*7*). This agreement suggests that our experimental conditions do not adversely affect protein structure and ligand binding properties. In the case of F293W/Wless, the red-shifted form may be an inactive structure of *lac* repressor that has vanishing IPTG affinity, and its formation may be induced by cryosolvent and/or reduced temperature or present, as well, at ambient temperatures in the absence of cryosolvent.

SUMMARY

The triplet-state properties of four single-tryptophan mutants of *lac* repressor protein and their complexes with the inducer sugar IPTG have been investigated by phosphorescence and ODMR spectroscopy. These single tryptophan residues are located in the core region of the protein, associated with the inducer binding pocket (W201Y and F293W/Wless) or located in its vicinity (Y273W/Wless) or in the monomer−monomer interface (H74W/Wless). Previous fluorescence studies have shown (*7*) that the environment surrounding the tryptophan residues at these locations in the protein is influenced by conformational changes caused by inducer binding. The investigation described here reveals large changes in the triplet-state properties of each of these tryptophan residues as a result of inducer binding, except for W220 (present in W201Y) in which only minor changes are observed; these data are in agreement with earlier fluorescence results. Furthermore, the environmental changes deduced by ODMR for the single tryptophans examined are consistent with environmental changes anticipated on the basis of the positions of the tryptophan residues examined in the structure of the repressor protein. This work demonstrates the sensitivity of the triplet state of tryptophan to changes in the local environment that result from a conformational change in protein structure.

REFERENCES

1. Miller, J. H., and Reznikoff, W. S. (1980) *The Operon*, 2nd ed., Cold Spring Harbor Laboratory Press, Cold Spring Harbor, NY.
2. Jobe, A., and Bourgeois, S. (1972) *J. Mol. Biol. 69*, 397−408.

3. Lin, S.-Y., and Riggs, A. D. (1975) *Cell 4*, 107−111.
4. Matthews, K. S., and Nichols, J. C. (1998) *Prog. Nucl. Acid Res. Mol. Biol. 58*, 127−164.
5. Lewis, M., Chang, G., Horton, N. C., Kercher, M. A., Pace, H. C., Schumacher, M. A., Brennan, R. G., and Lu, P. (1996) *Science 271*, 1247−1254.
6. Friedman, A. M., Fischmann, T. O., and Seitz, T. A. (1995) *Science 268*, 1721−1727.
7. Barry, J. K., and Matthews, K. S. (1997) *Biochemistry 36*, 15632−15642.
8. McGlynn, S. P., Azumi, T., and Kinoshita, M. (1969) *Molecular Spectroscopy of the Triplet State*, Prentice-Hall, Englewood Cliffs, NJ.
9. Purkey, R. M., and Galley, W. C. (1970) *Biochemistry 9*, 3569−3575.
10. Clarke, R. H., Ed. (1982) *Triplet State ODMR Spectroscopy*, Wiley-Interscience, New York.
11. Maki, A. H. (1995) *Methods Enzymol. 246*, 610−638.
12. Burns, L. E., Maki, A. H., Spotts, R., and Matthews, K. S. (1993) *Biochemistry 32*, 12821−12829.
13. Chakerian, A. E., and Matthews, K. S. (1991) *J. Biol. Chem. 266*, 22206−22214.
14. Kunkel, T. A. (1985) *Proc. Natl. Acad. Sci. U.S.A. 82*, 488−492.
15. Gardner, J. A., and Matthews, K. S. (1990) *J. Biol. Chem. 265*, 21061−21067.
16. Sommer, H., Lu, P., and Miller, J. H. (1976) *J. Biol. Chem. 251*, 3774−3779.
17. O'Gorman, R. B., Dunaway, M., and Matthews, K. S. (1980) *J. Biol. Chem. 255*, 10100−10106.
18. Chen, J., and Matthews, K. S. (1992) *J. Biol. Chem. 267*, 13843−13850.
19. Wu, J. Q., Ozarowski, A., and Maki, A. H. (1996) *J. Magn. Reson., Ser. A 119*, 82−89.
20. Schmidt, J., Veeman, W. S., and van der Waals (1969) *Chem. Phys. Lett. 4*, 341.
21. Ozarowski, A., Wu, J. Q., and Maki, A. H. (1996) *J. Magn. Reson., Ser. A 121*, 178−186.
22. Galley, W. C., and Purkey, R. M. (1970) *Proc. Natl. Acad. Sci. U.S.A. 67*, 1116−1121.
23. Ugurbil, K., Maki, A. H., and Bersohn, R. (1977) *Biochemistry 16*, 901−907.
24. Wu, J. Q., Ozarowski, A., Maki, A. H., Urbaneja, M. A., Henderson, L. E., and Casas-Finet, J. R. (1997) *Biochemistry 36*, 12506−12518.
25. Davis, J., and Maki, A. H. (1984) *Biochemistry 23*, 6249−6256.
26. Hershberger, M. V., Maki, A. H., and Galley, W. C. (1980) *Biochemistry 19*, 2204−2209.
27. Kleina, L. G., and Miller, J. H. (1990) *J. Mol. Biol. 212*, 295−318.
28. Wu, J. Q., Ozarowski, A., and Maki, A. H. (1997) *J. Phys. Chem. A 101*, 6177−6183.
29. Carson, M. (1987) *J. Mol. Graphics 5*, 103−106.
30. Wu, J. Q., Ozarowski, A., Davis, S. K., and Maki, A. H. (1996) *J. Phys. Chem. 100*, 11496−11503.

BI990242F